



Since January 2020 Elsevier has created a COVID-19 resource centre with free information in English and Mandarin on the novel coronavirus COVID-19. The COVID-19 resource centre is hosted on Elsevier Connect, the company's public news and information website.

Elsevier hereby grants permission to make all its COVID-19-related research that is available on the COVID-19 resource centre - including this research content - immediately available in PubMed Central and other publicly funded repositories, such as the WHO COVID database with rights for unrestricted research re-use and analyses in any form or by any means with acknowledgement of the original source. These permissions are granted for free by Elsevier for as long as the COVID-19 resource centre remains active.



Investigating the potential antiviral activity drugs against SARS-CoV-2 by molecular docking simulation

A.N. El-hoshoudy

Computational Chemistry Group, Egyptian Petroleum Research Institute, 11727 Nasr City, Cairo, Egypt

ARTICLE INFO

Article history:

Received 19 May 2020

Received in revised form 19 July 2020

Accepted 31 July 2020

Available online 4 August 2020

Keywords:

COVID-19

Coronavirus

Molecular docking

SARS-CoV-2

Homology modeling

ABSTRACT

Recently, scary viral pneumonia is known as (COVID-19) has swept the whole world. The new virus strain designated as SARS-CoV-2 belonging to the coronavirus family. Although the current medical research directed towards the development of a novel therapeutic agent, no anti-viral drug approved until now. On the medical scale, the development of an approved drug is a time-consuming process, so research is directed towards screening of ligands and drugs multimodal structure-based-design and then docked to the main viral protease to investigate the active binding sites. The bioinformatic approaches used to evaluate the competence of a comprehensive range of ligands and drugs before their clinical implementation. In this study, a computational approach through molecular docking simulation is conducted for screening the antiviral activity of drugs, natural sources, and inhibitory compounds against the SARS-CoV-2 genome. The main virus protease was collected from a Protein Data Bank (PDB# 6YB7) and docked with a sequence of 19 approved antiviral drugs, 10 natural inhibitory ligands against COVID-19 downloaded from PubChem, in addition to 10 natural sources optimized for *Escherichia coli* BL₂₁ (DE₃) to identify the antiviral activity of these candidates against COVID-19. The docking results were promised and indicated that the reported ligands can firmly bind to the SARS-CoV-2 main protease and leads to inhibition of its infectious impact.

© 2020 Elsevier B.V. All rights reserved.

1. Introduction

The recent world history is punctuated by the appearance of highly pathogenic three coronaviruses which cause human fatal pneumonia including severe acute respiratory syndrome coronavirus (SARS-CoV), Middle-East respiratory syndrome coronavirus (MERS-CoV), and SARS-CoV-2 [1,2]. The SARS-CoV epidemic in 2002 and the MERS-CoV epidemic in 2012 proved that coronaviruses would traverse the barrier to species and develop as severe pathogenic viruses [3]. Coronaviruses (CoVs), are divided into four genera, α -, β -, δ - and γ -coronaviruses [4]. SARS-CoV-2 is a member of β -coronaviruses which subdivided into A, B, C, and D lineages [5]. Robson [6] defined SARS-CoV-2 viral protein as a strain of human SARS [7]. SARS-CoV-2 which synonymously known as (COVID-19) virus was commenced in the late of December 2019 [7–9] as an outbreak of pneumonia with a mysterious etiological agent responsible for the viral pneumonia outbreak that swept the world [4,8,10–19], and created a significant threat to the global community health [4]. On 30th, January 2020 the World Health Organization (WHO) announced that COVID-19 epidemic a global health crisis of international interest [2,20,21]. On 14th, March 2020, the disease infect 81,026 people in China, with a case fatality ratio of 3.9% (3194/81026)

[22]. The number of victims increases incrementally and can be monitored by the WHO statistics website (<https://www.who.int/emergencies/diseases/novel-coronavirus-2019>). Respiratory globules and direct communication are traditional transmission routes for SARS-CoV-2 [23]. Common infection symptoms include respiratory distress, malaise, fever, dry cough, dyspnea, and shortness of breath [8,14]. In advanced serious cases, the infection can cause pneumonia, kidney failure, severe acute respiratory disorder, and even death [1]. The remedies of coronavirus infection involve inhibition of the synthesis of viral RNA through prohibiting the virus's genetic material, inhibiting virus replication, and blocking the virus binding to human cell receptors or inhibiting the virus's self-assembly process through acting on some structural proteins [1]. Coronaviruses (CoVs) comprise two characteristic proteins; 1) structural proteins which include Spike (S), Nucleocapsid (N), Membrane (M) that spans the membrane, and Envelope (E) proteins which are a hydrophobic protein that covers the entire structure of the coronavirus [24]; and 2) non-structural proteins which include proteases (nsp3 and nsp5) and RdRp (nsp12) [14,25]. The transmembrane spike (S) glycoprotein forms homotrimers projecting from the virion envelope surface [26] and promotes viral entry into the host cell [1,27] in addition to facilitating the binding of the host and viral tissues [28]. The S protein is a single-chain comprises of about 1300 amino acids [7] and subdivided into two functional subunits (S1 and S2). The S1 subunit has a receptor-binding domain

E-mail address: azizchemist@yahoo.com.

(RBD) that binds with high affinity to host cell receptor (angiotensin-converting enzyme 2; ACE-2 protein) which considered the key determinant of virus contagiousness [2,29–31]. After fusion, the S2 subunit has the N-terminal domain (NTD) [31] responsible for binding between the virus and cellular host cell membrane [32]. The virus entry into the host cell requires the cleavage of S1-S2 subunits at the boundary to reveal S2 for combination to the cell membrane [2,32,33]. For all coronaviruses, the S protein is further cleaved by host proteases [34]. S trimers are densely decorated by heterogeneous N-linked glycans protruding from the trimer surface and important for proper folding and

modulating availability to host proteases and neutralizing antibodies [2,35,36]. SARS-CoV-2 is an enveloped, positive single RNA strand coronavirus with a genome sequence ranging from 26.0 to 32.0 kilobases [37–39]. On 10th January 2020, the viral genome was released on NCBI GenBank. The first high-resolution crystal structure of SARS-CoV-2 main protease released on February 5th, 2020 on Protein Data Bank (PDB) Doi: <https://doi.org/10.2310/pdb6lu7/pdb> [1,2,7]. 6LU7 is the monomer of the main protease in the active state with the N3 peptidomimetic inhibitor [40]. On 25th March 2020, 6YB7 released as SARS-CoV-2 main protease with unliganded active site (2019-nCoV,

Table 1
Summary of the approved antiviral drugs.

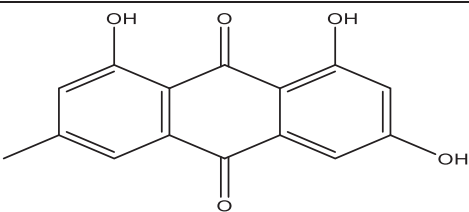
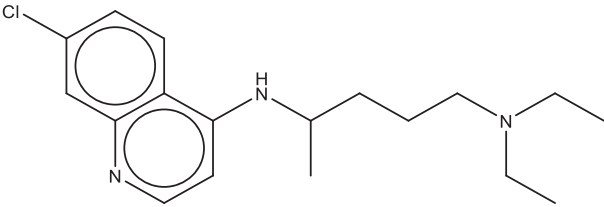
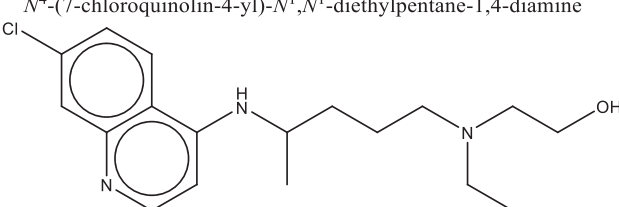
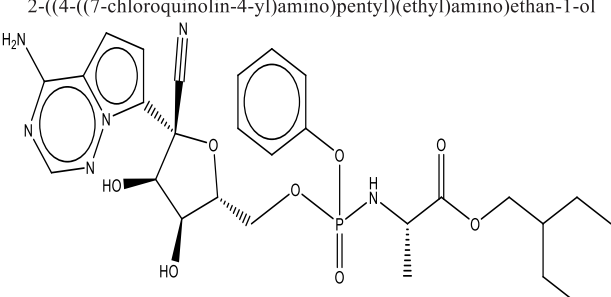
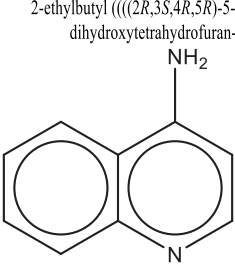
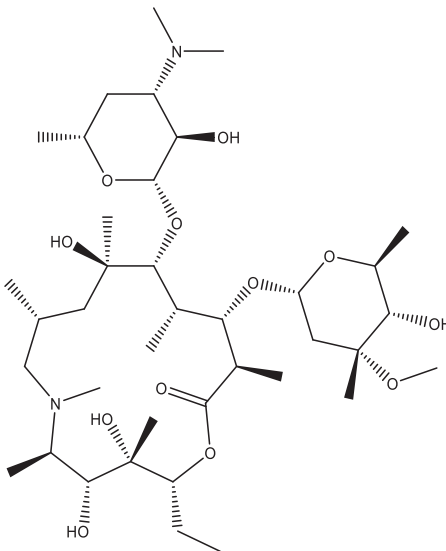
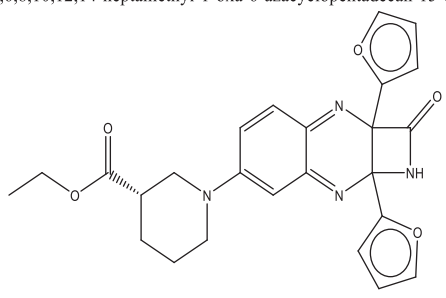
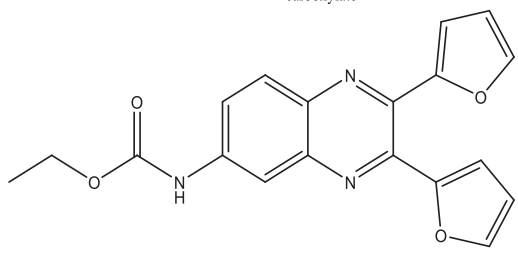
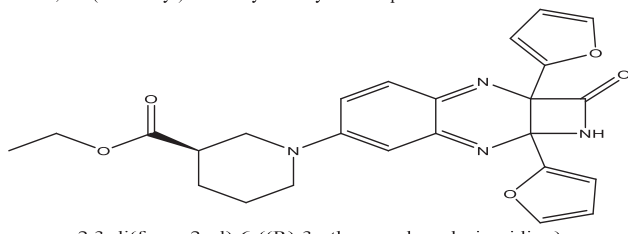
#	Cpd.	Structure/IUPAC name	Biological activity
1	Emodin	 1,3,8-trihydroxy-6-methylanthraquinone	Inhibitor of SARS-CoV entry [7]
2	Chloroquine	 <i>N</i> ⁴ -(7-chloroquinolin-4-yl)- <i>N</i> ¹ , <i>N</i> ¹ -diethylpentane-1,4-diamine	Treatment of SARS-CoV-2 [45]
3	hydroxychloroquine	 <i>N</i> ⁴ -(7-chloroquinolin-4-yl)- <i>N</i> ¹ , <i>N</i> ¹ -diethylpentane-1,4-diamine-3-ol	Treatment of SARS-CoV-2 [45]
4	Remdesivir	 2-((4-((7-chloroquinolin-4-yl)amino)pentyl)(ethyl)amino)ethan-1-ol	Antiviral drug [46]
5	Aminoquinoline	 quinolin-4-amine	Used in malaria treatment [9]

Table 1 (continued)

#	Cpd.	Structure/IUPAC name	Biological activity
6	Azithromycin	 <p>(2<i>R</i>,3<i>S</i>,4<i>R</i>,5<i>R</i>,8<i>R</i>,10<i>R</i>,11<i>R</i>,12<i>S</i>,13<i>S</i>,14<i>R</i>)-11-(((2<i>S</i>,3<i>R</i>,4<i>S</i>,6<i>R</i>)-4-(dimethylamino)-3-hydroxy-6-methyltetrahydro-2<i>H</i>-pyran-2-yl)oxy)-2-ethyl-3,4,10-trihydroxy-13-(((2<i>R</i>,4<i>R</i>,5<i>S</i>,6<i>S</i>)-5-hydroxy-4-methoxy-4,6-dimethyltetrahydro-2<i>H</i>-pyran-2-yl)oxy)-3,5,6,8,10,12,14-heptamethyl-1-oxa-6-azacyclopentadecan-15-one</p>	Broad spectrum antibiotic [12]
7	ethyl (3 <i>S</i>)-1-(2 <i>a</i> ,8 <i>a</i> -di(furan-2-yl)-2-oxo-1,2,2 <i>a</i> ,8 <i>a</i> -tetrahydroazeto[2,3- <i>b</i>]quinoxalin-6-yl)piperidine-3-carboxylate	 <p>ethyl (3<i>S</i>)-1-(2<i>a</i>,8<i>a</i>-di(furan-2-yl)-2-oxo-1,2,2<i>a</i>,8<i>a</i>-tetrahydroazeto[2,3-<i>b</i>]quinoxalin-6-yl)piperidine-3-carboxylate</p>	Cyclophilin D (CypD) inhibitors [47]
8	2,3-di(furan-2-yl)-6-ethoxycarbonylamino quinoxaline	 <p>2,3-di(furan-2-yl)-6-ethoxycarbonylamino quinoxaline</p>	
9	2,3-di(furan-2-yl)-6-((<i>R</i>)-3-ethoxycarbonyl-piperidino) carbonylamino quinoxaline	 <p>2,3-di(furan-2-yl)-6-((<i>R</i>)-3-ethoxycarbonyl-piperidino) carbonylamino quinoxaline</p>	

(continued on next page)

Table 1 (continued)

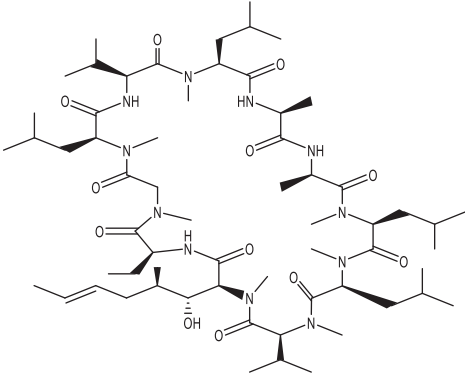
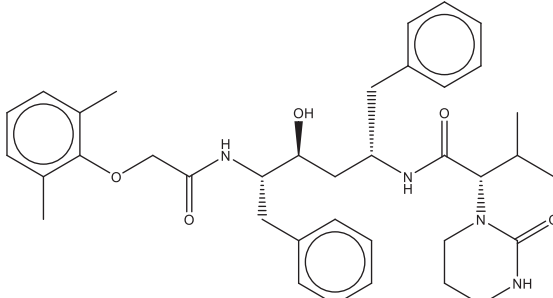
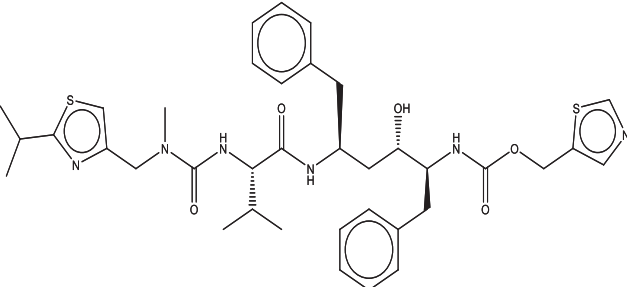
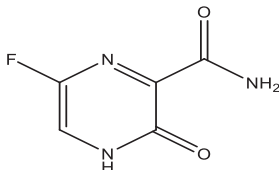
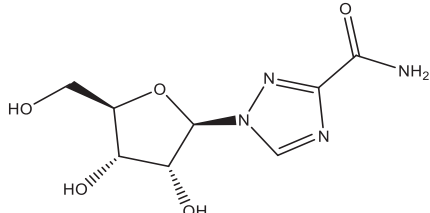
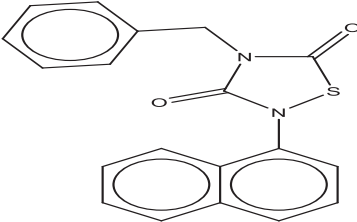
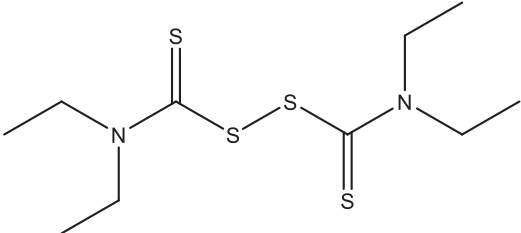
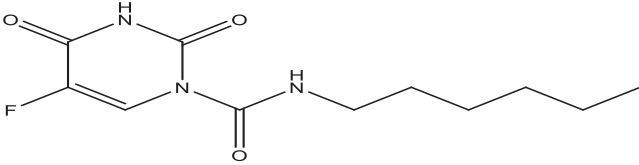
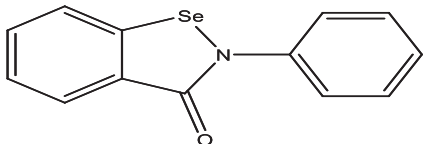
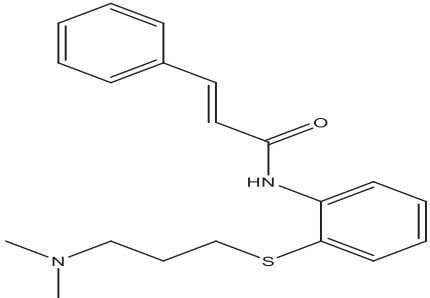
#	Cpd.	Structure/IUPAC name	Biological activity
10	Cyclosporine A	 <p>(3<i>S</i>,6<i>S</i>,9<i>S</i>,12<i>R</i>,15<i>S</i>,18<i>S</i>,21<i>S</i>,24<i>S</i>,30<i>S</i>,33<i>S</i>)-30-ethyl-33-((1<i>R</i>,2<i>R</i>,<i>E</i>)-1-hydroxy-2-methylhex-4-en-1-yl)-6,9,18,24-tetraisobutyl-3,21-diisopropyl-1,4,7,10,12,15,19,25,28-nonamethyl-1,4,7,10,13,16,19,22,25,28,31-undecaazacyclotriactan-2,5,8,11,14,17,20,23,26,29,32-undecaone</p>	In vitro effective against HIV, HCV and HBV replication [48,49]
11	Lopinavir	 <p>(<i>S</i>)-<i>N</i>-((2<i>S</i>,4<i>S</i>,5<i>S</i>)-5-(2-(2,6-dimethylphenoxy)acetamido)-4-hydroxy-1,6-diphenylhexan-2-yl)-3-methyl-2-(2-oxotetrahydropyrimidin-1(2<i>H</i>)-yl)butanamide</p>	(HIV protease inhibitors) [4]
12	Ritonavir	 <p>thiazol-5-ylmethyl ((2<i>S</i>,3<i>S</i>,5<i>S</i>)-3-hydroxy-5-(<i>S</i>)-2-(3-(2-isopropylthiazol-4-yl)methyl)-3-methylureido)-3-methylbutanamide)-1,6-diphenylhexan-2-yl)carbamate</p>	
13	Favipiravir	 <p>6-fluoro-3-oxo-3,4-dihydropyrazine-2-carboxamide</p>	SARS-CoV-2 antiviral agent [4]
14	Ribavirin	 <p>1-((2<i>R</i>,3<i>R</i>,4<i>S</i>,5<i>R</i>)-3,4-dihydroxy-5-(hydroxymethyl)tetrahydrofuran-2-yl)-1<i>H</i>-1,2,4-triazole-3-carboxamide</p>	HCV antiviral [37]

Table 1 (continued)

#	Cpd.	Structure/IUPAC name	Biological activity
15	Tideglusib	 4-benzyl-2-(naphthalen-1-yl)-1,2,4-thiadiazolidine-3,5-dione	Antiviral agent [10]
16	Disulfiram		FDA-approved drugs [10]
17	Carmofur	 5-fluoro-N-hexyl-2,4-dioxo-3,4-dihydropyrimidine-1(2H)-carboxamide	
18	Ebselen	 2-phenylbenzo[d][1,2]selenazol-3(2H)-one	Currently in clinical trials [10]
19	Cinanserin	 N-(2-((3-(dimethylamino)propylthio)phenyl)cinnamamide	Antiviral drug [10]

coronavirus disease 2019, COVID-19) DOI: <https://doi.org/10.2210/pdb6YB7/pdb>. Although the current medical research proceeds urgently to diagnose active antiviral agents that can inhibit the pandemic spread of the novel viral infection, no targeted/approved therapeutic drug or vaccine has been accredited till now as it is a time-consuming process [1,10,31,41]. Consequently, the swift approach relies on the use of computational programs of combined structure-assisted drug design, bioinformatics, and drug screening [10,42], in addition to the development of a predictive 3D protein structures of SARS-CoV-2 has become very crucial to identify new inhibitory drugs for SARS-CoV-2 protease [7,43]. Roboson [7] stated the usage of the Q-UEL computational method to simulate the inhibition efficiency of some drugs on COVID-19. In this work, the author conducting a computational approach, through applying a combination of virtual screening, and molecular docking

techniques, to assess the ability of some potential drugs, inhibitory ligands and natural products for the non-covalent inhibition of the SARS-CoV-2 main protease [40] through conformational and molecular docking studies. Molecular docking allows quick identification of the amino acid sequences across many coronaviruses including SARS-CoV-2 [7,44]. The obtained docking results were hopeful and proposed a potential inhibition against the newly emerged COVID-19 from the presently accessible therapeutics [1].

2. Materials and reagents

All the screened drugs, inhibitory ligands, and natural product structures were built up from their smile format in ChemBioDraw 2019 software. All the molecules were energy minimized before molecular

Table 2
Summary of the natural sources optimized for *Escherichia coli* BL₂₁ (DE₃).

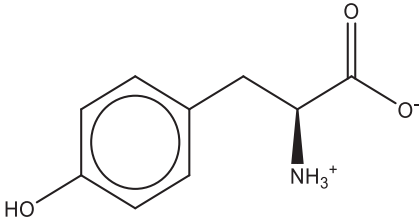
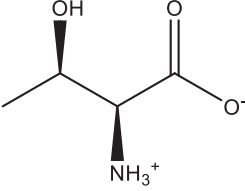
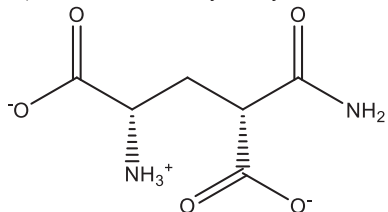
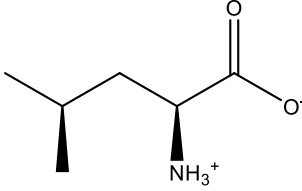
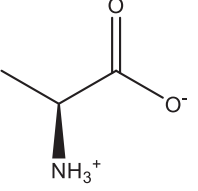
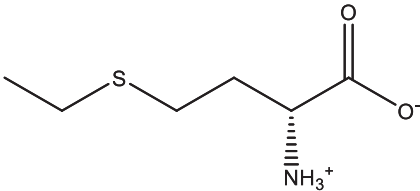
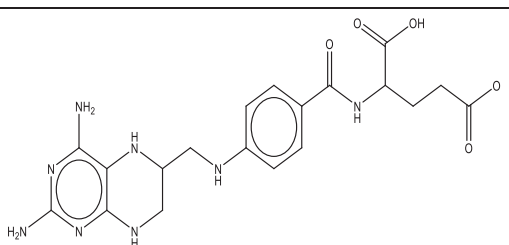
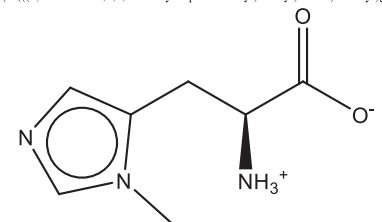
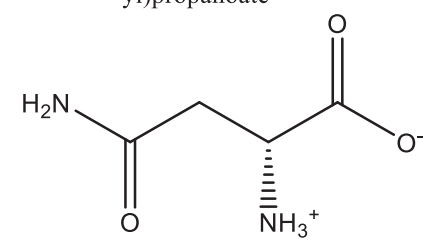
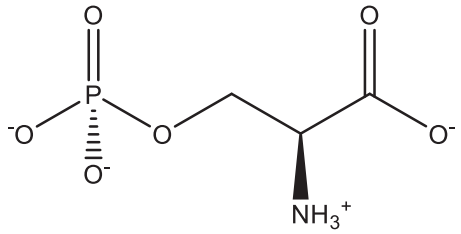
#	Natural Cpd. name	Serial No.	Structure/IUPAC name
1	L-tyrosine zwitterion	SN0000130	 <p>(<i>S</i>)-2-ammonio-3-(4-hydroxyphenyl)propanoate</p>
2	L-threonine zwitterion	SN00001733	 <p>(2<i>S</i>,3<i>R</i>)-2-ammonio-3-hydroxybutanoate</p>
3	(2 <i>S</i> ,4 <i>R</i>)-2-ammonio-4-carbamoylpentanedioate	SN00160264	 <p>(2<i>S</i>,4<i>R</i>)-2-ammonio-4-carbamoylpentanedioate</p>
4	L-leucine	SN00003439	 <p>(<i>S</i>)-2-ammonio-4-methylpentanoate</p>
5	L-alanine zwitterion	SN00011326	 <p>(<i>S</i>)-2-ammoniopropanoate</p>
6	(2 <i>R</i>)-2-ammonio-4-(ethylsulfanyl)butanoate	SN00002388	 <p>(<i>R</i>)-2-ammonio-4-(ethylthio)butanoate</p>

Table 2 (continued)

#	Natural Cpd. name	Serial No.	Structure/IUPAC name
7	(4-(((2,4-diamino-5,6,7,8-tetrahydropteridin-6-yl)methyl)amino)benzoyl)glutamic acid	SN00193091	 (4-(((2,4-diamino-5,6,7,8-tetrahydropteridin-6-yl)methyl)amino)benzoyl)glutamic acid
8	(2S)-2-ammonio-3-(3-methylimidazol-4-yl)propanoate	SN00001765	 (S)-2-ammonio-3-(1-methyl-1H-imidazol-5-yl)propanoate
9	D-asparagine	SN00156119	 (R)-4-amino-2-ammonio-4-oxobutanoate
10	O-phosphonato-L-serine(2-)	SN00005709	 (S)-2-ammonio-3-(phosphonooxy)propanoate

docking simulation [31]. The screened compounds comprise three categories divided as follows; 19 approved antiviral drugs presently available on the market and have been authorized for use against a variety of viruses. 10 natural inhibitors ligands against COVID-19 were downloaded from PubChem (<https://pubchem.ncbi.nlm.nih.gov/#query=coronavirus&tab=compound&page=4>) and selected according to H-bond donor count, and 10 natural compounds selected from the natural sources site available at http://bioinf-applied.charite.de/supernatural_new/index.php?site=pathway&organism=ebe&pathway_type=Genetic%20Information%20Processing. The full-length gene encoding COVID-19 virus was optimized for *Escherichia coli* BL21 (DE3) expression [10]. Tables 1–3 summarize the structure of the compounds for the three categories respectively.

2.1. Sequence alignment and homology modeling

The recently emerged SARS-CoV-2 nucleotide gene was retrieved from the protein data bank (PDB ID: 6YB7, chain A) since it is the last approved SARS-CoV-2 main protease during the editing of this manuscript. 6YB7 is the monomer of the main protease with the unliganded active site [40]. The sequence was downloaded as a PDB format. 6YB7 is SARS-CoV-2 main protease with 306 sequence length and 1.25 Å resolution. The protein sequence stated in Table 4, while the crystal 3D structure of COVID-19 main protease shown in Fig. 1. The model validated after the addition of missed hydrogen atoms to prepare the protonated 3D-structure for the docking study [14]. After validation, the systems were energy-minimized [50] to obtain a fully optimized and

Table 3
Summary of inhibitory ligands against COVID-19 downloaded from the PubChem.

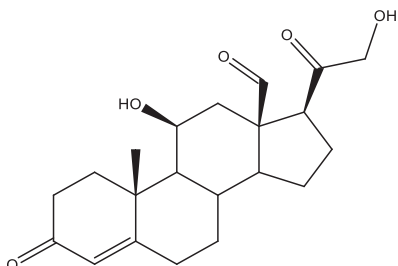
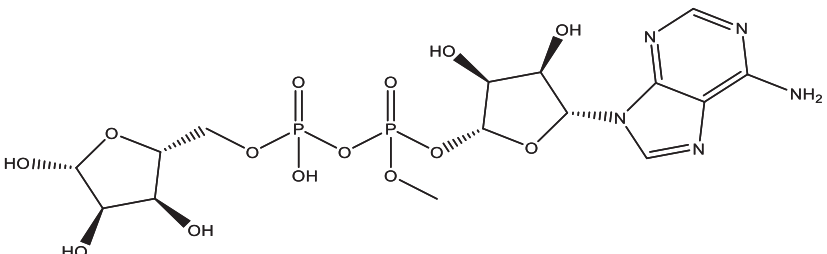
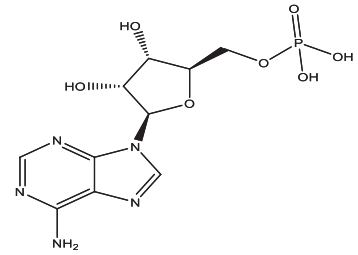
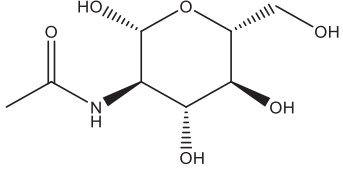
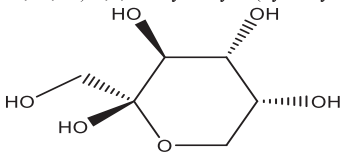
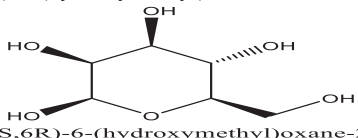
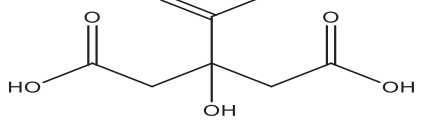
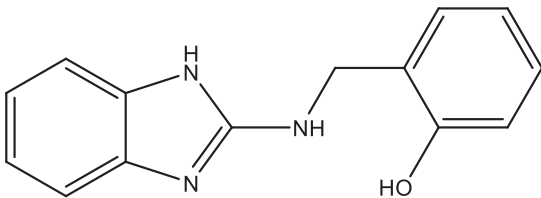
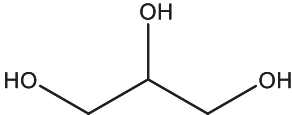
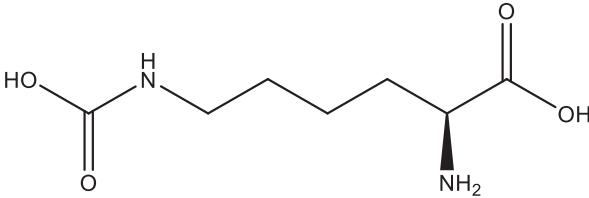
#	Compound CID	Structure/IUPAC name
1	24758425	 <p>(10R,11S,13R,17S)-11-hydroxy-17-(2-hydroxyacetyl)-10-methyl-3-oxo-1,2,6,7,8,9,11,12,14,15,16,17-dodecahydrocyclopenta[a]phenanthrene-13-carbaldehyde</p>
2	445794	 <p>[[[(2R,3S,4R,5R)-5-(6-aminopurin-9-yl)-3,4-dihydroxyoxolan-2-yl]methoxy-hydroxyphosphoryl][(2R,3S,4R,5R)-3,4,5-trihydroxyoxolan-2-yl]methyl hydrogen phosphate</p>
3	6083	 <p>[(2R,3S,4R,5R)-5-(6-aminopurin-9-yl)-3,4-dihydroxyoxolan-2-yl]methyl dihydrogen phosphate</p>
4	24139	 <p>N-[(2R,3R,4R,5S,6R)-2,4,5-trihydroxy-6-(hydroxymethyl)oxan-3-yl]acetamide</p>
5	24310	 <p>(2R,3S,4R,5R)-2-(hydroxymethyl)oxane-2,3,4,5-tetrol</p>
6	439680	 <p>(2R,3S,4S,5S,6R)-6-(hydroxymethyl)oxane-2,3,4,5-tetrol</p>
7	311	 <p>2-hydroxypropane-1,2,3-tricarboxylic acid</p>

Table 3 (continued)

#	Compound CID	Structure/IUPAC name
8	787400	 2-[(1H-benzimidazol-2-ylamino)methyl]phenol
9	753	 propane-1,2,3-triol
10	17754054	 (2S)-2-amino-6-(carboxyamino)hexanoic acid

stable structure for further docking simulation. Energy minimization carried out using Amber10: EHT forcefield with current forcefield charges applied to all atoms, R-field solvation, cutoff (8,10 Å), and distance-dependent dielectric constant of 4.0 [47]. Amber parameters applied for nucleic acid, and EHT parameters applied for small molecules. The system conducted in a triclinic non-periodic cell (1.P1) with a size of $10 \times 10 \times 10$ and cell shape $90 \times 90 \times 90$. The constraints including rigid water molecules with a gradient of 0.1 RMS kcal/mol/Å². Docked complexes were subsequently submitted to iterative cycles of 500 maximum iterations with a gradient of 0.01, radius offset of 0.4, and one minimization cycle [47].

2.2. Molecular docking simulation

In this study, the SARS-CoV-2 main protease was retrieved from the protein data bank (PDB ID: 6YB7, chain A) [14]. After model validation, alignment of the protein sequences, and subsequent molecular docking conducted to evaluate the antiviral effect of the previously reported drugs, and natural sources against SARS-CoV-2 protease. The binding energies and the inhibition constants are reported in each case [44]. All of the compounds were optimized in their active physiological settings [51]. Before testing the ligands against SARS-CoV-2 protease, the structures of the tested drugs and ligands were ensured to be in the optimized active arrangement. Finally, the ligands selected based on analyzing the predicted binding modes and their scores [10].

3. Results and discussion

Compounds with lower molecular docking scores will have higher binding correspondences with the target 6YB7 protein [1]. The orientation of a ligand is evaluated with a shape-scoring function which approximates the binding energies of the ligand-receptor. The shape-scoring function is an empirical function resembling the van der Waals' attractive energy. After the initial orientation and scoring evaluation, energy minimization is conducted to pinpoint the closest energy minimization points within the receptor-binding sites [47]. Most of the tested ligands (39 ligands) including the 19 antiviral drugs, 10 natural inhibitory ligands, and 10 natural sources optimized for *Escherichia coli* bear hydrogen bond acceptors or donors [40] and exhibit excessive H-bonding, π - π interaction and/or hydrophobic interaction with the 6YB7 protease as summarized in Tables 5–7. These electrostatic interactions imply that these ligands are potent inhibitors for the SARS-CoV-2 protease [1], since, the formed complex between the screened ligands and SARS-CoV-2 main protease is highly stable with higher binding energies. The formation of excessive hydrogen bonding with the main protease chain indicates the ability of the ligand to lock the virus-binding receptor [10]. By analyzing the docking results, it's found that **Ritonavir** antiviral drug, [(2R,3S,4R,5R)-5-(6-aminopurin-9-yl)-3,4-dihydroxyoxolan-2-yl]methoxyhydroxyphosphoryl [(2R,3S,4R,5R)-3,4,5-trihydroxyoxolan-2-yl]methyl hydrogen phosphate (**Cpd. CID (445794)**), and (4-(((2,4-diamino-5,6,7,8-tetrahydropteridin-6-yl)methyl)amino)benzoyl)glutamic acid (**Cpd. Serial No.# SN00193091**)

Table 4

Sequence structure of SARS-CoV-2 main protease.

QUERY: Sequence = SGFRKMAFPSPGKVEGCMVQVTCGTTTLNGLWLDVVYCPRHVICTSEDMLNPNYEDLLIRKSNHNFVQAGNVQLRVIGHSMQNCVLLKLVDTANPKTPKYKFVRIQPGQT FSVLACYNGSPSGVYQCAMRPNFTIKGSFLNGSCGVSFGFNIDYDCVDFCYMHMELPTGVHAGTDLEGNFYGPFVDRQTAQAAGTDTTITVNVLAWLYAAVINGDRWFLNRFITTLNDFNLVAMK YNYPELTQDHDVILGPLSAQTGIAVLDMCASLKELLQNGMNGRTILGSALLEDEFTPFVDRQCSGVTFQ

AND Target = Protein **AND E-Value Cutoff** = 1,000,000 **AND Identity Cutoff** = 0

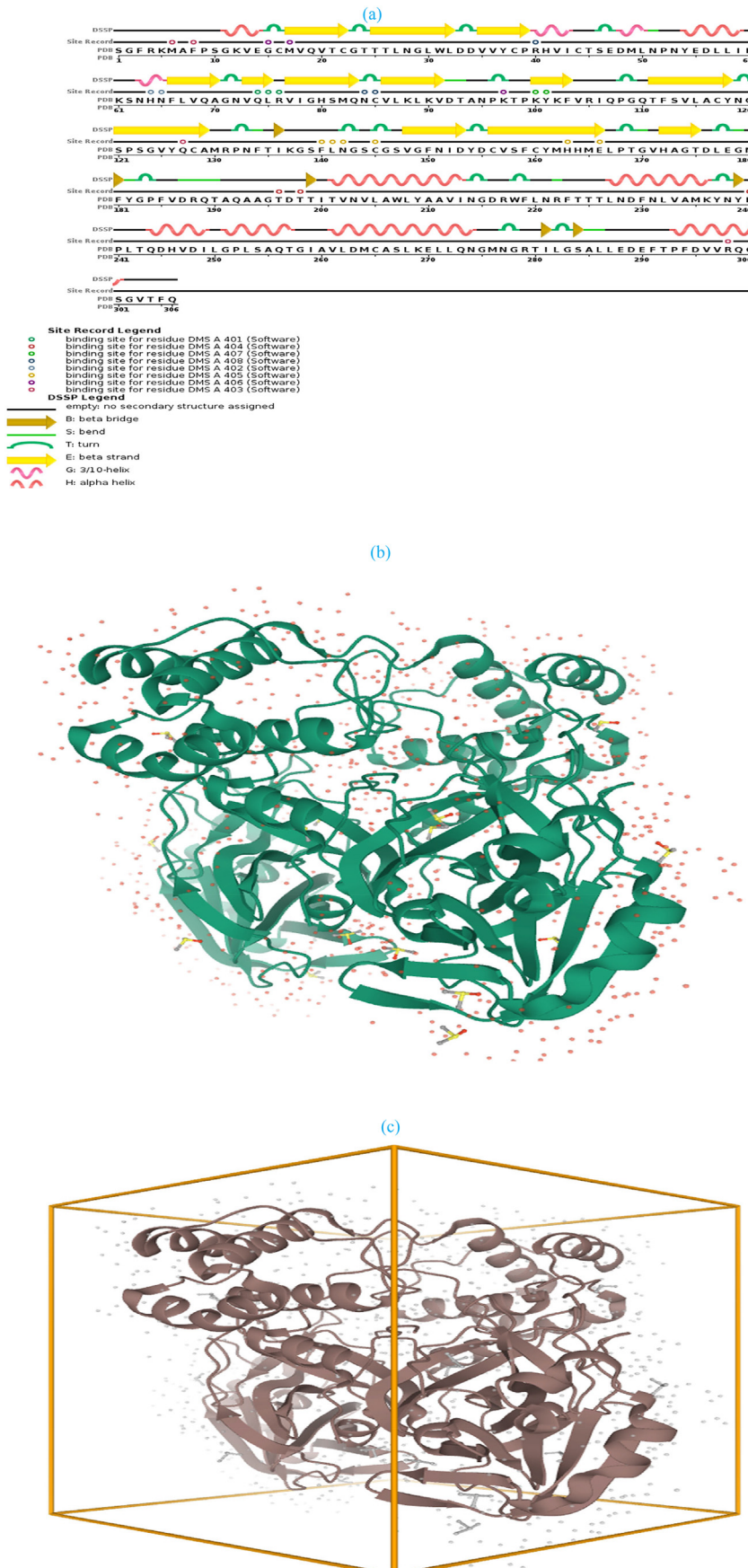
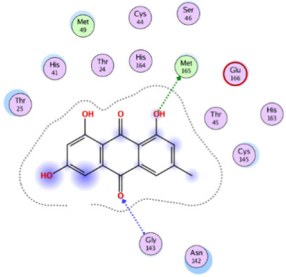
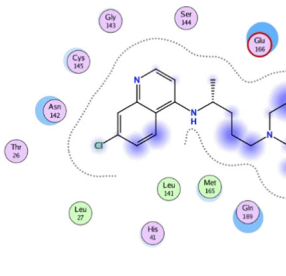
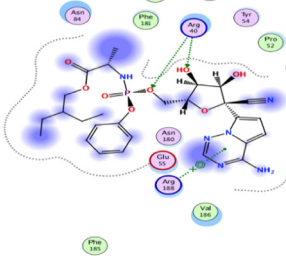
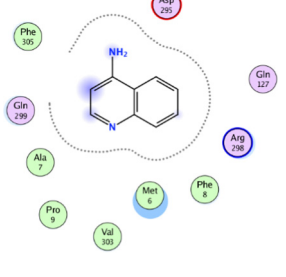
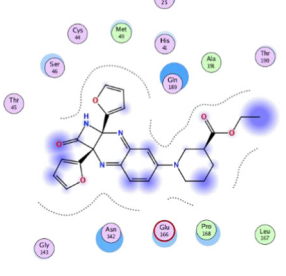


Fig. 1. (a) Cladogram representation of SARS-CoV-2 main protease; (b) 6YB7-SARS-CoV-2 main protease with unliganded active site (c) crystal 3D structure of 6YB7- main protease.

Table 5

Summary of docking interactions in case of the antiviral drugs.

#	Cpd. name	Docking interaction	Docking score	Interpretation
1	Emodin		-5.37	H-bond with Met165, π - π bonding with Gly143
2	Chloroquine		-5.95	
3	Remdesivir		-7.12	2-H bonding with Arg40, arene cation bonding between Arg188 and pyrrole ring
4	Aminoquinoline		-5.21	
5	Ethyl (3S)-1-(2a,8a-di(furan-2-yl)-2-oxo-1,2,2a,8a-tetrahydroazeto[2,3-b]quinoxalin-6-yl)piperidine-3-carboxylate		-6.30	

(continued on next page)

Table 5 (continued)

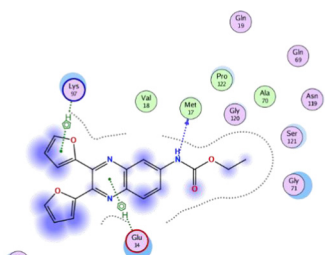
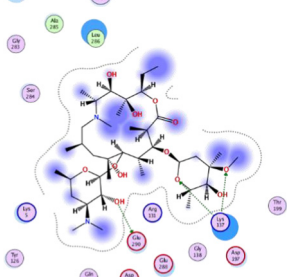
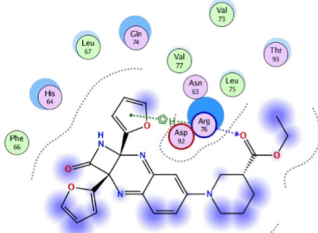
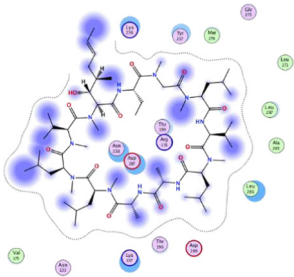
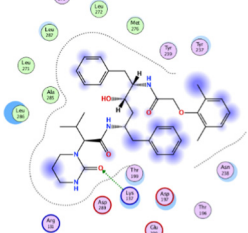
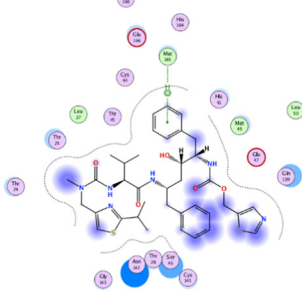
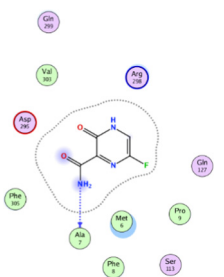
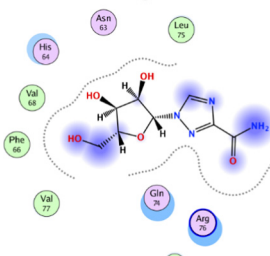
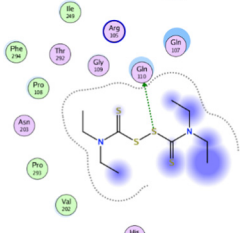
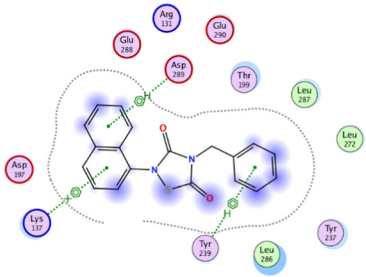
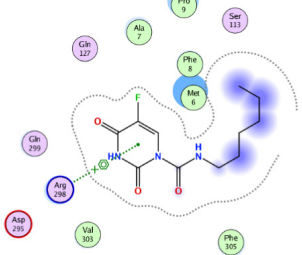
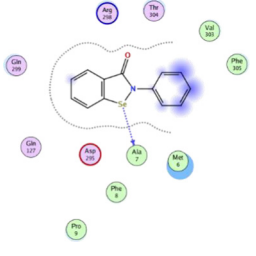
#	Cpd. name	Docking interaction	Docking score	Interpretation
6	2,3-di(furan-2-yl)-6-ethoxycarbonylamino quinoxaline		-5.99	H-bonding with Met17, arene-h-bonding between Glu14 and pyridazine ring, arene-H-bonding between Lys97 and furan ring
7	Azithromycin		-6.58	3-H-bonding with lys137 and Glu290
8	Ethyl (3S)-1-(2a,8a-di(furan-2-yl)-2-oxo-1,2,2a,8a-tetrahydroazeto [2,3-b]quinoxalin-6-yl) piperidine-3-carboxylate		-6.61	Arene-H-bonding with Arg76, Asp92
9	Cyclosporine A		-7.81	Excessive π - π interaction with Asn218, Asp197, Thr199, and Arg131
10	Lopinavir		-7.57	π - π interaction with Lys137
11	Ritonavir		-8.12	Arene-H-bonding with Met165

Table 5 (continued)

#	Cpd. name	Docking interaction	Docking score	Interpretation
12	Favipiravir		-4.95	H-bonding with Ala7
13	Ribavirin		-5.05	
14	Disulfiram		-5.40	π - π interaction with Gln110
15	Tideglusib		-5.95	2-Arene-h interaction with Asp289&Tyr239, one Arene-cation bonding with Lys137.
16	Carmofur		-6.53	Arene-cation interaction with Arg298
17	Ebselen		-5.90	π - π interaction between Se and Ala7

(continued on next page)

Table 5 (continued)

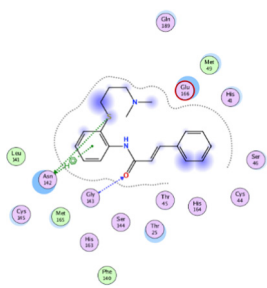
#	Cpd. name	Docking interaction	Docking score	Interpretation
18	Cinanserin		-6.72	π - π interaction and Arene-H bonding with Asn142 & Gly143
19	Hydroxychloroquine		-5.86	

Table 6Summary of interactions in case of natural sources optimized for *Escherichia coli* BL₂₁ (DE₃).

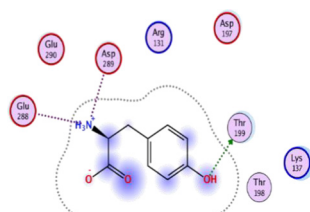
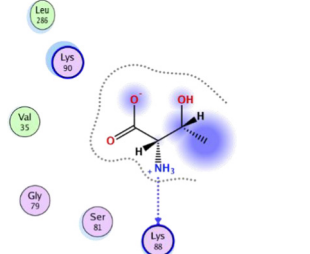
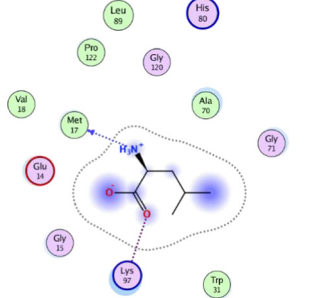
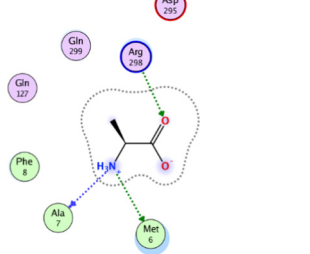
#	Cpd. name	Docking interaction	Docking score	Interpretation
1	L-tyrosine zwitterion		-4.21	3-H-bonding with Thr199, Glu288, and Asp289
2	L-threonine zwitterion		-3.94	H-bonding with Lys88
3	L-leucine		-3.98	π - π bonding with Lys97, H-bonding with Met17
4	L-alanine zwitterion		-4.01	2-H-bonding with Ala7, Met6, and π - π interaction with Arg298

Table 6 (continued)

#	Cpd. name	Docking interaction	Docking score	Interpretation
5	(2R)-2-ammonio-4-(ethylsulfanyl)butanoate		-4.15	H-bonding with Glu288,290, Asp289, π - π interaction with Lys137, Asp197
6	(2S,4R)-2-ammonio-4-carbamoylpentanedioate		-4.12	Anion-anion and π - π interactions with Lys137, Arg131, 3-H-bonding with Glu288, 290, Asp289
7	4-(((2,4-diamino-5,6,7,8-tetrahydropteridin-6-yl)methyl)amino)benzoyl glutamic acid		-7.17	π - π interaction with Gly71
8	(2S)-2-ammonio-3-(3-methylimidazol-4-yl)propanoate		-4.14	2-H-bonding with Thr199, Asp289
9	D-asparagine		-3.84	Anion-anion and π - π interactions with Lys137, Arg131, 3-H-bonding with Leu287, Asp289, Glu290
10	O-phosphonato-L-serine(2-)		-3.91	Anion-anion interaction with Lys88, 90

Table 7
Summary of interactions in case of natural inhibitory ligands against COVID-19 downloaded from PubChem.

#	Cpd. CID	Docking interaction	Docking score	Interpretation
1	753		-4.02	H-bonding with Met6
2	787400		-5.20	H-bonding with Thr199
3	24758425		-5.84	
4	311		-4.30	2-H-bonding with Leu287, Asp197 π - π interactions with Lys137, Asp289
5	17754054		-4.86	π - π interaction with Gly71, 2-H-bonding with Met17, Lys97
6	6083		-5.46	π - π interaction with Lys90, H-bonding with Gln83

Table 7 (continued)

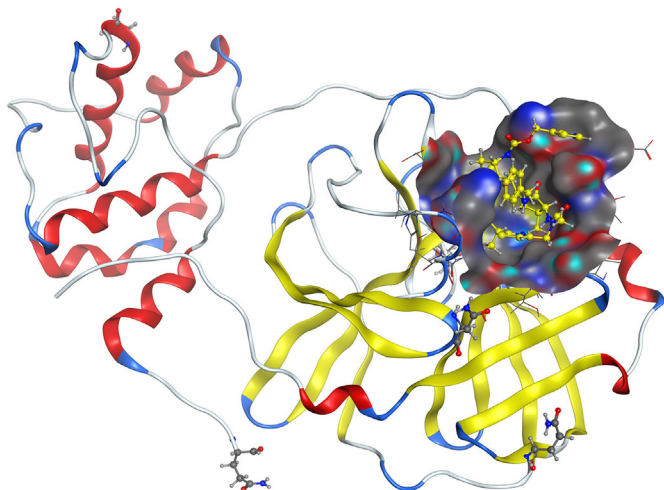
#	Cpd. CID	Docking interaction	Docking score	Interpretation
7	24139		-4.86	π - π interaction with Lys97, 2-H-bonding with Met17, Glu14
8	24310		-4.96	4-H-bonding with Met6, Arg298
9	439,680		-5.07	5-H-bonding with Gln299, Asp295, Met6
10	445794		-6.39	2-H-bonding with Leu287, Asp197

exhibits the highest binding affinity, in case of the antiviral drugs, inhibitory ligands, and natural sources optimized for *Escherichia coli* with binding energies of -8.12 , -6.39 , -7.17 , kcal/mol, respectively. The docking results indicate that these ligands can bind tightly to the new COVID-19 protease and disorder the polymerase function. Consequently, these ligands are potent inhibiting candidates for 6YB7 main protease of the SARS-CoV-2. Fig. 2a–c illustrates the highest three ligands interaction with their surface maps successively, while other ligands–6YB7 protease interactions are provided in supplementary data (Tables S1–S3). Based on the binding energies and docking scores, **Ritonavir** antiviral drug considered as the strongest inhibiting agent rather than other screened 39 ligands with a higher binding energy of -8.12 kcal/mol. Furthermore, **Ritonavir** found to have a strong binding pattern with aromatic moieties, so it is the most potent docked ligands [40]. The docking study exhibited that the screened ligands inhibit coronaviruses and illuminate the road for medical scientists to develop in-vivo and in-vitro compounds against COVID-19.

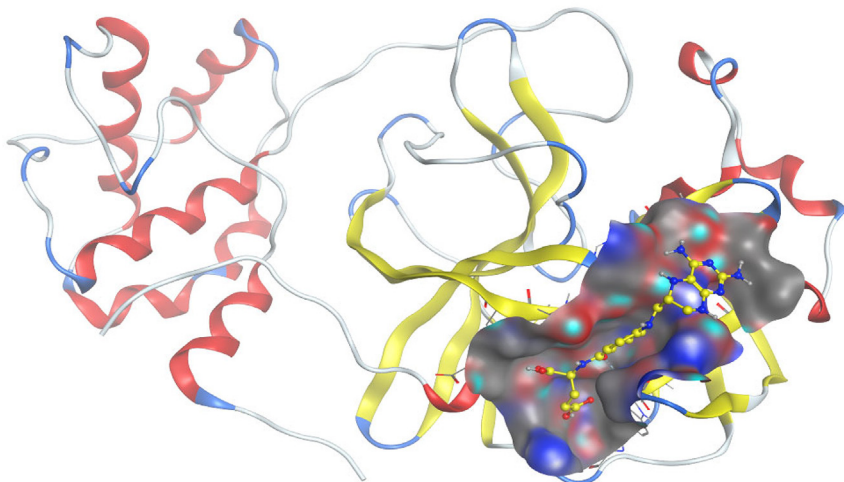
4. Conclusion

The newly emerged COVID-19 virus is a serious health concern in the 20th century. Although there is a sequence of medical drugs and natural products demonstrated high binding affinity to various viral proteins, the development of an in-vivo and in-vitro medical inhibitory drug for SARS-CoV-2 is a challenging and time-consuming task. As a result, in silico and bioinformatic routes is a fast way to assess an effective drug against SARS-CoV-2. A rigorous computational docking was pursued to identify the antiviral activity of any drug before medical usage. The present study screened the inhibitory effect of 39 ligands based on molecular docking of 6YB7 protease. The docking results exhibited that the reported ligands exhibit a high binding affinity to the COVID-19 protease and can inhibit its viral infection. Ritonavir antiviral drug binds to SARS-CoV-2 main protease with a score of -8.12 , so it is expected that ritonavir is a potent inhibitor for SARS-CoV-2 pneumonia. The results obtained in this study are based on computer docking

(a) Ritonavir antiviral drug



(b) (4-(((2,4-diamino-5,6,7,8-tetrahydropteridin-6-yl)methyl)amino)benzoyl)glutamic acid (Cpd. Serial No.# SN00193091)



(c) [[[2R,3S,4R,5R)-5-(6-aminopurin-9-yl)-3,4-dihydroxyoxolan-2-yl]methoxyhydroxyphosphoryl] [(2R,3S,4R,5R)-3,4,5-trihydroxyoxolan-2-yl]methyl hydrogen phosphate (Cpd. CID (445794))

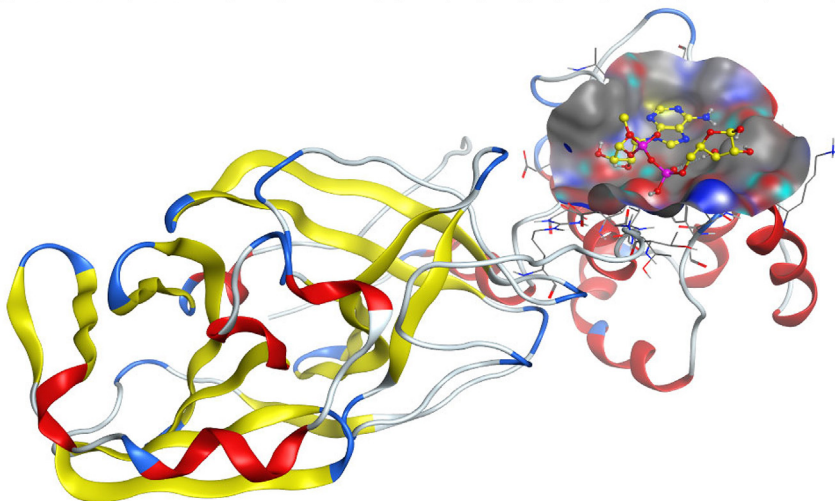


Fig. 2. Ligands interaction with their surface maps.

simulation, and no in vivo and in vitro anti-viral assessment conducted till now, since the author aims to share these results with medical scientists to face SARS-CoV-2 epidemic urgently.

CRedit authorship contribution statement

A.N. El-hoshoudy: Conceptualization, Data curation, Formal analysis, Funding acquisition, Investigation, Methodology, Project administration, Resources, Software, Supervision, Validation, Visualization, Writing - original draft, Writing - review & editing.

Declaration of competing interest

The authors declare that they have no known competing for financial interests or personal relationships that could have appeared to influence the work reported in this paper.

Appendix A. Supplementary data

Supplementary data to this article can be found online at <https://doi.org/10.1016/j.molliq.2020.113968>.

References

- [1] C. Wu, Y. Liu, Y. Yang, P. Zhang, W. Zhong, Y. Wang, Q. Wang, Y. Xu, M. Li, X. Li, *Acta Pharm. Sin. B* 10 (5) (2020) 766–788.
- [2] A.C. Walls, Y.-J. Park, M.A. Tortorici, A. Wall, A.T. McGuire, D. Velesler, *Cell* 181 (2) (2020) 281–292.e6.
- [3] S. Perlman, *Mass Medical Soc.*, 2020.
- [4] S. Xia, M. Liu, C. Wang, W. Xu, Q. Lan, S. Feng, F. Qi, L. Bao, L. Du, S. Liu, *Cell Res.* (2020) 1.
- [5] I.M. Ibrahim, D.H. Abdelmalek, M.E. Elshahat, A.A. Elfiky, *J. Inf. Secur.* 80 (5) (2020) 554–562.
- [6] B. Robson, Possible Importance of the KRSPFDLLFNKV Motif, Circulated and Published on ResearchGate [Google Scholar], 2010.
- [7] B. Robson, *Comput. Biol. Med.* (2020) 103670.
- [8] D.S. Hui, E.I. Azhar, T.A. Madani, F. Ntoumi, R. Kock, O. Dar, G. Ippolito, T.D. Mchugh, Z.A. Memish, C. Drosten, *Int. J. Infect. Dis.* 91 (2020) 264.
- [9] Z. Sahræi, M. Shabani, S. Shokouhi, A. Saffæi, *Int. J. Antimicrob. Agents* (2020), 105945.
- [10] Z. Jin, X. Du, Y. Xu, Y. Deng, M. Liu, Y. Zhao, B. Zhang, X. Li, L. Zhang, C. Peng, *bioRxiv* (2020) <https://doi.org/10.1038/s41586-020-2223-y>.
- [11] M. Tobaiqy, M. Qashqary, S. Al-Dahery, A. Mujallad, A.A. Hershan, M.A. Kamal, N. Helmi, *Infection Prevention in Practice* (2020) 100061.
- [12] P. Gautret, J.-C. Lagier, P. Parola, L. Meddeb, M. Mailhe, B. Doudier, J. Courjon, V. Giordanengo, V.E. Vieira, H.T. Dupont, *Int. J. Antimicrob. Agents* 56 (1) (2020), 105949.
- [13] C.-C. Lai, T.-P. Shih, W.-C. Ko, H.-J. Tang, P.-R. Hsueh, *Int. J. Antimicrob. Agents* (2020) 105924.
- [14] A.A. Elfiky, *Life Sci.* (2020) 117592.
- [15] I.I. Bogoch, A. Watts, A. Thomas-Bachli, C. Huber, M.U. Kraemer, K. Khan, *J. Travel Med.* 27 (2) (2020) 1–3.
- [16] H.A. Rothan, S.N. Byrareddy, *J. Autoimmun.* (2020) 102433.
- [17] C. Huang, Y. Wang, X. Li, L. Ren, J. Zhao, Y. Hu, L. Zhang, G. Fan, J. Xu, X. Gu, *Lancet* 395 (2020) 497.
- [18] N. Zhu, D. Zhang, W. Wang, X. Li, B. Yang, J. Song, X. Zhao, B. Huang, W. Shi, R. Lu, *New Engl. J. Med.* 382 (2020) 727–733.
- [19] F. Wu, S. Zhao, B. Yu, Y.-M. Chen, W. Wang, Z.-G. Song, Y. Hu, Z.-W. Tao, J.-H. Tian, Y.-Y. Pei, *Nature* 579 (2020) 265.
- [20] V.M. Corman, O. Landt, M. Kaiser, R. Molenkamp, A. Meijer, D.K. Chu, T. Bleicker, S. Brünink, J. Schneider, M.L. Schmidt, *Eurosurveillance* 25 (2020), 2000045.
- [21] L.-s. Wang, Y.-r. Wang, D.-w. Ye, Q.-q. Liu, *Int. J. Antimicrob. Agents* (2020) 105948.
- [22] C. Zhang, Z. Wu, J.-W. Li, H. Zhao, G.-Q. Wang, *Int. J. Antimicrob. Agents* (2020) 105954.
- [23] W. Shang, Y. Yang, Y. Rao, X. Rao, *npj Vaccines* 5 (2020) 1.
- [24] T. Pillaiyar, M. Manickam, V. Namasivayam, Y. Hayashi, S.-H. Jung, *J. Med. Chem.* 59 (2016) 6595.
- [25] A.A. Elfiky, S.M. Mahdy, W.M. Elshemey, *J. Med. Virol.* 89 (2017) 1040.
- [26] M.A. Tortorici, A.C. Walls, Y. Lang, C. Wang, Z. Li, D. Koerhuis, G.-J. Boons, B.-J. Bosch, F.A. Rey, R.J. de Groot, *Nat. Struct. Mol. Biol.* 26 (2019) 481.
- [27] S. Belouzard, J.K. Millet, B.N. Licitra, G.R. Whittaker, *Viruses* 4 (2012) 1011.
- [28] F. Li, *Annual Review of Virology* 3 (2016) 237.
- [29] R.N. Kirchdoerfer, N. Wang, J. Pallesen, D. Wrapp, H.L. Turner, C.A. Cottrell, K.S. Corbett, B.S. Graham, J.S. McLellan, A.B. Ward, *Sci. Rep.* 8 (2018) 1.
- [30] W. Song, M. Gui, X. Wang, Y. Xiang, *PLoS Path.* 14 (2018), e1007236.
- [31] J. Fantini, C. Di Scala, H. Chahinian, N. Yahi, *Int. J. Antimicrob. Agents* 55 (5) (2020), 105960.
- [32] A.B. FB, F. Sarialioglu, *Med. Hypotheses* 142 (2020), 109743.
- [33] D. Wrapp, N. Wang, K.S. Corbett, J.A. Goldsmith, C.-L. Hsieh, O. Abiona, B.S. Graham, J.S. McLellan, *Science* 367 (2020) 1260.
- [34] J.K. Millet, G.R. Whittaker, *Virus Res.* 202 (2015) 120.
- [35] A.C. Walls, X. Xiong, Y.-J. Park, M.A. Tortorici, J. Snijder, J. Quispe, E. Cameroni, R. Gopal, M. Dai, A. Lanzavecchia, *Cell* 176 (2019) 1026.
- [36] X. Xiong, M.A. Tortorici, J. Snijder, C. Yoshioka, A.C. Walls, W. Li, A.T. McGuire, F.A. Rey, B.-J. Bosch, D. Velesler, *J. Virol.* 92 (2018), e01628.
- [37] A. Shannon, N.T.T. Le, B. Selisko, C. Eydoux, K. Alvarez, J.-C. Guillemot, E. Decroly, O. Peersen, F. Ferron, B. Canard, *Antivir. Res.* (2020) 104793.
- [38] S. Kumar, 2020 (2020).
- [39] H. Nishiura, S.-m. Jung, N.M. Linton, R. Kinoshita, Y. Yang, K. Hayashi, T. Kobayashi, B. Yuan, A.R. Akhmetzhanov, *Multidisciplinary Digital Publishing Institute*, 2020.
- [40] M. Macchiagodena, M. Pagliari, P. Procacci, *Chem. Phys. Lett.* (2020) 137489.
- [41] C.A. Lipinski, F. Lombardo, B.W. Dominy, P.J. Feeney, *Adv. Drug Del. Rev.* 23 (1997) 3.
- [42] C. Perricone, P. Triggianese, E. Bartoloni, G. Cafaro, A.F. Bonifacio, R. Bursi, R. Perricone, R. Gerli, *J. Autoimmun.* (2020) 102468.
- [43] S. Kumar, *BMC Res. Notes* 8 (2015) 9.
- [44] K.N. Chitralla, X. Yang, B. Busbee, N.P. Singh, L. Bonati, Y. Xing, P. Nagarkatti, M. Nagarkatti, *Sci. Rep.* 9 (1) (2019).
- [45] P. Colson, J.-M. Rolain, J.-C. Lagier, P. Brouqui, D. Raoult, *Int. J. Antimicrob. Agents* (2020), 105932.
- [46] M. Wang, R. Cao, L. Zhang, X. Yang, J. Liu, M. Xu, Z. Shi, Z. Hu, W. Zhong, G. Xiao, *Cell Res.* 30 (2020) 269.
- [47] H.X. Guo, F. Wang, K.Q. Yu, J. Chen, D.L. Bai, K.X. Chen, X. Shen, H.L. Jiang, *Acta Pharmacol. Sin.* 26 (2005) 1201.
- [48] A. Ahmed-Belkacem, L. Colliandre, N. Ahnou, Q. Nevers, M. Gelin, Y. Bessin, R. Brillet, O. Cala, D. Douguet, W. Bourguet, *Nat. Commun.* 7 (1) (2016).
- [49] S. Hopkins, P.A. Gallay, *Biochimica et Biophysica Acta (BBA)-General Subjects* 1850 (2015) 2103.
- [50] M. Batool, M. Shah, M.C. Patra, D. Yesudhas, S. Choi, *Sci. Rep.* 7 (2017) 1.
- [51] A.A. Elfiky, A. Ismail, *Life Sci.* 238 (2019) 116958.